# Microcavity semiconductor laser with enhanced spontaneous emission

Y. Yamamoto and S. Machida
*NTT Basic Research Laboratories, Musashino-shi, Tokyo 180, Japan*

G. Björk
*Department of Microwave Engineering, The Royal Institute of Technology, S-10044, Stockholm, Sweden*
(Received 22 August 1990)

A metal-clad optical waveguide with a semiconductor microcavity structure is proposed to increase the coupling efficiency of spontaneous emission into a lasing mode (spontaneous emission coefficient $\beta$) and to increase a total spontaneous emission rate simultaneously. Such a microcavity semiconductor laser with enhanced spontaneous emission has novel characteristics, including high quantum efficiency, low threshold pump rate, broad modulation bandwidth, and intensity noise reduced to below the shot-noise limit (amplitude squeezing).

## I. INTRODUCTION

Spontaneous emission is a remarkable manifestation of the interaction between an atom and vacuum fields. The role of vacuum fields in driving an excited atom to its ground state is often disregarded, and spontaneous emission is sometimes erroneously regarded as being an inherent feature in the behavior of atoms. However, it has been demonstrated theoretically[1] and experimentally[2] that the radiative properties of an atom can be altered by modifying the vacuum-field fluctuations using a cavity wall. The rate of spontaneous emission depends on the density of electromagnetic modes and the local-field intensity of vacuum fluctuation. Spontaneous emission is inhibited if the cavity is off resonant and/or if the atom is located at a node of a mode function, and is enhanced if the cavity is resonant and/or the atom is located at an antinode of a mode function.[3] Inhibited and enhanced spontaneous emission has been successfully observed at microwave frequencies.[4–6]

Inhibited and enhanced spontaneous emission has also been observed at optical frequencies using a cavity wall.[7–9] It also has been demonstrated experimentally[10] and theoretically[11] that the rate of spontaneous emission is altered by a dielectric constant of a medium, in which an atom is located. This is because both the density of modes and the vacuum field intensity are modulated by a dielectric constant.

Such capability of modifying spontaneous emission by a cavity wall holds technological promise for realizing an efficient laser.[12–14] This paper shows that a threshold pump rate can be decreased substantially by increasing the coupling efficiency of spontaneous emission into a lasing mode. To increase modulation bandwidth, the spontaneous emission lifetime must be decreased. If the increased coupling efficiency of spontaneous emission and the decreased spontaneous lifetime are realized simultaneously, the intensity noise can be suppressed to below the shot-noise level (amplitude squeezing) at broad pumping range and at broad frequency range.

However, vacuum-field alteration at optical frequencies is much more difficult than at microwave frequencies, because a superconducting cavity does not exist at optical frequencies. A metal-clad optical cavity has a large absorption loss. A dielectric three-dimensional periodic structure has been proposed to alter vacuum-field fluctuations and to realize a stop band at optical frequencies.[15] However, fabrication of such a complex microcavity structure requires difficult microfabrication technologies. A dielectric one-dimensional periodic structure, which can be fabricated easily, can have a high coupling efficiency of spontaneous emission into a cavity resonant mode, but its spontaneous lifetime cannot be shortened.[16] Spontaneous emission rate at microwave frequencies is enchanced just above the cutoff in a superconductor waveguide.[3] This property has been proposed to decrease the spontaneous emission lifetime at optical frequencies.[17] However, a normal metal has a fairly large resistive absorption loss at optical frequencies and the mode at just above its cutoff does not feature such cavity-enhanced spontaneous emission due to high absorption loss.[18,19]

The paper proposes an alternative microcavity structure that achieves high coupling efficiency into a lasing mode and a short lifetime of spontaneous emission simultaneously. The proposed structure is based on a semiconductor-core–metal-clad optical waveguide with a buffer layer, in which a low-loss fundamental transverse mode well above the cutoff is resonated by a microcavity structure formed inside the semiconductor-core region.

This paper also demonstrates novel characteristics of such a microcavity-structured semiconductor laser, which includes reduction of threshold current, increase in direct modulation bandwidth, and decrease in intensity noise below shot-noise level (amplitude squeezing).

## II. BRIEF REVIEW ON THE COUPLING EFFICIENCY AND THE LIFETIME OF SPONTANEOUS EMISSION IN CONVENTIONAL SEMICONDUCTOR LASERS

### A. Spontaneous emission pattern and lifetime

Let us consider a dipole moment along the $x$ axis in polar coordinates $(r,\psi,\phi)$ as shown in Fig. 1. The dipole

 

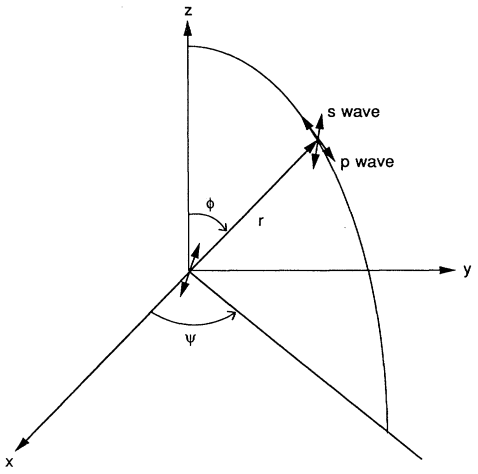


FIG. 1. Polar coordinates $(r,\psi,\phi)$ for radiation pattern calculation.

emits electromagnetic fields with polarizations both perpendicular ($s$ wave) and parallel ($p$ wave) to the emission plane. The radiation intensity at the point $(r,\psi,\phi)$ is[2]

$$dI(r,\psi,\phi)=\eta\frac{P_{12}^2E_0^2}{r^2}\times\begin{cases}\sin^2\psi, & s \text{ wave}\\ \cos^2\psi\cos^2\phi, & p \text{ wave}\end{cases}. \tag{2.1}$$

Here $\eta$ is a constant, $P_{12}$ is the dipole moment, and $E_0^2$ is the vacuum-field intensity at the location ($r=0$) of the dipole moment. In conventional semiconductor lasers with a large active volume embedded in a homogeneous semiconductor medium, $E_0^2$ is independent of $\psi$ and $\phi$. That is, the vacuum-field fluctuation is isotropic. The total emitted intensity is given by

$$I\equiv\int_0^{2\pi}d\psi\int_0^{\pi}d\phi\, r^2(\sin\phi)dI(r,\psi,\phi)=\tfrac{8}{3}\pi\eta P_{12}^2E_0^2 . \tag{2.2}$$

Of this total intensity, three-quarters is radiated as the $s$ wave and one-quarter as the $p$ wave.

If the dipole moment is along the $y$ axis, the result is exactly the same. However, if the dipole moment is along the $z$ axis, the radiation intensity at the point $(r,\psi,\phi)$ is[2]

$$dI(r,\psi,\phi)=\eta\frac{P_{12}^2E_0^2}{r^2}\times\begin{cases}0, & s \text{ wave}\\ \sin^2\phi, & p \text{ wave}\end{cases}. \tag{2.3}$$

The total emitted intensity,

$$I\equiv\int_0^{2\pi}d\psi\int_0^{\pi}d\phi\, r^2(\sin\phi)dI(r,\psi,\phi)=\tfrac{8}{3}\pi\eta P_{12}^2E_0^2 , \tag{2.4}$$

is the same as in (2.2) for the dipole moment along the $x$ axis, as it should be; however, in this case, all the emitted power is carried by the $p$ wave. Therefore, if a number of dipoles have moments that are randomly oriented, i.e., if the dipole moments are equally distributed along the $x$, $y$, and $z$ axes, then the overall spontaneous emission intensities in the two polarizations are equal.

For a two-level atom, the spontaneous decay rate $\gamma$, which is equal to the inverse of the spontaneous lifetime, is proportional to the total emitted spontaneous intensity $I$ and is given by

$$\gamma^{\text{free}}=\frac{2\omega_0^2P_{12}^2}{3\pi\hbar c^3} , \tag{2.5}$$

for free space. If the two-level atom is located in a homogeneous medium with a dielectric constant $\epsilon$, both the local vacuum-field intensity and the density of modes are altered and the new spontaneous decay rate is given by[11]

$$\gamma^{\text{diel}}=\frac{9\epsilon^{5/2}}{(2\epsilon+1)^2}\gamma^{\text{free}} . \tag{2.6}$$

The spontaneous decay rate of a minority carrier in semiconductors is quite different from that of a two-level atom. The conduction electrons and the valence holes have the distributions of $\rho_c(E')f(E')$ and $\rho_v(E'')[1-f(E'')]$, respectively. The spontaneous decay rate is not only dependent on the dipole moment and the dielectric constant but also dependent on the concentration of a majority carrier. The spontaneous decay rate in a semiconductor for the negligible minority-carrier density as compared with majority-carrier concentration is given by $\gamma=Bp$, where $p$ is the background doping of majority carriers.

The spontaneous emission rate $\gamma$ in semiconductors is proportional to the total emitted spontaneous intensity $I$ and is given by[20]

$$\gamma=Bp\propto\int_{-\infty}^{\infty}\rho_c(E')\rho_v(E'')|P_{12}(E',E'')|^2\times f(E')[1-f(E'')]dE' . \tag{2.7}$$

Here the photon energy $E$ is equal to the difference of the energies of the conduction electron $E'$ and the valence hole $E''$. The dipole moment $P_{12}$ depends on the energies $E_1$ and $E_2$. When injected minority-carrier density $n$ greatly exceeds the background doping $p$, the spontaneous lifetime $\tau_{\text{sp}}=1/\gamma$ is given by $1/Bn$ instead of $1/Bp$. $B$ is on the order of $3\times10^{-10}$ cm$^{-3}$ s$^{-1}$ for a GaAs semiconductor and so the spontaneous lifetime is on the order of 3 ns at $n\simeq10^{18}$ cm$^{-3}$.[20]

### B. Coupling efficiency $\beta$ of spontaneous emission into a lasing mode

Suppose an active volume $V$ of a semiconductor laser, which is much larger than the cube of optical wavelength, is enclosed by "perfect reflectors." The number of modes per unit frequency interval is given by $8\pi\nu^2V\epsilon^{3/2}/c^3$. If we assume that active dipoles are distributed uniformly in the volume $V$ and are randomly oriented, the coupling efficiency of spontaneous emission into each mode is identical. The total spontaneous emission rate is given by

$$R_{\text{sp}}\equiv N_c\gamma=\int\frac{8\pi\nu^2V\epsilon^{3/2}}{c^3}|g|^2\frac{2\Gamma N_c}{4\pi^2(\nu-\nu_0)^2+\Gamma^2}d\nu$$

$$=\frac{8\pi\nu^2V\epsilon^{3/2}|g|^2N_c}{c^3} . \tag{2.8}$$

Here $|g|^2$ is the electric dipole coupling constant and a Lorentzian line shape is assumed, $2\Gamma$ is the spontaneous emission linewidth in rad/s (FWHM), and $N_c$ is total

minority-carrier number. If the lasing frequency is coincident with gain center $\nu=\nu_0$, the spontaneous emission rate $E_{cv}$ into one lasing mode is

$$E_{cv}=\frac{2|g|^2N_c}{\Gamma} . \tag{2.9}$$

From (2.8) and (2.9), the coupling efficiency $\beta$ of spontaneous emission into the lasing mode (spontaneous emission coefficient) is calculated as[21]

$$\beta\equiv\frac{E_{cv}}{R_{\rm sp}}=\frac{c^3}{4\pi\nu^2\epsilon^{3/2}V\Gamma}=\frac{\lambda^4}{4\pi^2V\Delta\lambda\epsilon^{3/2}}\simeq 0.025\frac{\lambda^4}{\epsilon^{3/2}\Delta\lambda V} . \tag{2.10}$$

Here $\Delta\lambda=\lambda^2\Gamma/\pi c$ is the spontaneous emission linewidth in meters (FWHM).

The above argument is not based on an accurate model for a real semiconductor laser. In a real semiconductor laser, the spontaneous emission is partly coupled to several guided modes in an active waveguide and the rest is coupled to radiation continuum modes. The spontaneous emission radiated at angles $\theta$ larger than the critical angle $\theta_c$ of the total internal reflection at the active waveguide boundary is trapped in the waveguide as guided modes and that radiated at angles $\theta$ smaller than $\theta_c$ is lost as radiation modes, so that the coupling efficiency into the guided modes is approximately given by

$$\eta_g=\frac{\int_{\theta_c}^{\pi/2}(\sin^3\theta+\sin\theta+\sin\theta\cos^2\theta)d\theta}{\int_0^{\pi/2}(\sin^3\theta+\sin\theta+\sin\theta\cos^2\theta)d\theta}=\cos\theta_c . \tag{2.11}$$

The first terms inside the parentheses in the integrands above represent contributions from the $p$-wave vertical dipole, the second from the $s$-wave horizontal dipole, and the third from the $p$-wave horizontal dipole. Of the spontaneous emission coupled to the guided modes, only a small fraction is actually coupled to the single-lasing mode. Suppose the active waveguide supports only the fundamental transverse mode. The number of guided modes within the spontaneous emission spectral linewidth is then given by

$$M=2\frac{\Delta\lambda}{\Delta\lambda_c}=\frac{4\epsilon^{1/2}L\Delta\lambda}{\lambda^2} , \tag{2.12}$$

where the factor of 2 accounts for the two polarization directions, $\Delta\lambda_c=\lambda^2/2\epsilon^{1/2}L$ is the longitudinal mode separation, and $L$ is the cavity length. The single transverse mode waveguide has a cross-sectional area on the order of $A_{\rm eff}\sim\lambda^2/4\epsilon$, so that the cavity length $L$ is related to the active volume $V$ via $L=4\epsilon V/\lambda^2$. The coupling efficiency into the single lasing mode from all the guided modes is thus given by

$$\eta_l\equiv\frac{1}{M}=\frac{\lambda^4}{16\epsilon^{3/2}\Delta\lambda V} . \tag{2.13}$$

From (2.11) and (2.13), the spontaneous emission coefficient $\beta$ is

$$\beta\equiv\eta_g\eta_l=\frac{\lambda^4\cos\theta_c}{16\epsilon^{3/2}\Delta\lambda V} . \tag{2.14}$$

If the refractive index ratio $\mu_2/\mu_1$ of the active waveguide and cladding medium is about 0.92, which is typical in a GaAs semiconductor laser, then $\cos\theta_c\simeq 0.4$ and (2.14) reduces to

$$\beta\simeq 0.025\frac{\lambda^4}{\epsilon^{3/2}\Delta\lambda V} . \tag{2.15}$$

The two different models result in similar spontaneous emission coefficients $\beta$. If we use the numerical parameters of a typical GaAs semiconductor laser, $\lambda=8\times10^{-7}$ m, $\epsilon^{1/2}=3.5$, $\Delta\lambda=5\times10^{-8}$ m, and $V=4\times10^{-16}$ m$^3$, the spontaneous emission coefficient $\beta$ is on the order of $10^{-5}$. This means that only one photon out of $10^5$ spontaneously emitted photons is coupled into a lasing mode.

## III. MODIFIED SPONTANEOUS EMISSION IN A METAL-CLAD OPTICAL WAVEGUIDE MICROCAVITY

Let us consider a semiconductor-core–metal-clad optical waveguide, in which a microcavity structure is formed in a core region, as shown in Fig. 2. A semiconductor core region (post) has a half-wavelength or one-wavelength optical microcavity layer which is sandwiched by distributed Bragg reflectors. The distributed Bragg reflectors (DBR's) consist of two alternating quarter-wavelength layers with refractive indices of $\mu_1$ and $\mu_2$. A dielectric buffer layer exists between a semiconductor core region (post) and a metal cladding.

It is possible to make the fundamental transverse mode of the metal-clad waveguide be resonant for the microcavity. The conditions required for this is given by

$$\beta_0 d=\pi \text{ or } 2\pi \tag{3.1}$$

and

$$\beta_0' l_1=\beta_0'' l_2=\frac{\pi}{2} , \tag{3.2}$$

where $\beta_0$, $\beta_0'$, and $\beta_0''$ are the real parts of the propagation constants (phase constants) of the fundamental transverse mode in the half-wavelength (or one-wavelength) optical cavity layer with thickness $d$ and in the two DBR layers with thickness $l_1$ and $l_2$.

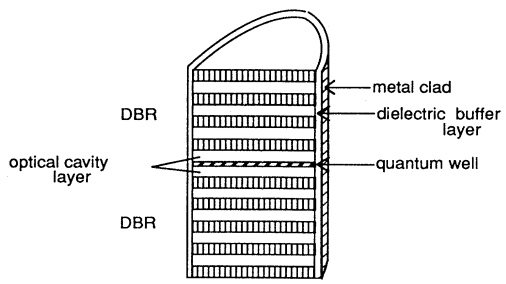


FIG. 2. A semiconductor-core–metal-clad optical waveguide with a microcavity structure.

It is also possible to make the surface-plasmon modes[18,19] and all the higher-order guided modes be off-resonant (either in the stopband of the microcavity or outside the stop band) if the waveguide cross section is not too large and if the spontaneous emission linewidth is not too broad. This situation is schematically shown in Fig. 3. The electric- and magnetic-field distributions of the fundamental and some higher-order modes of a metal-clad optical waveguide are schematically shown in Fig. 4. The phase constant $\beta_0$ of the fundamental transverse ($HE_{11}$) mode is given by

$$\beta_0=\frac{2\pi\mu_0}{c_0}(\nu^2-\nu_0^2)^{1/2}\ , \tag{3.3}$$

there $\mu_0$ is refractive index of the optical cavity layer and $\nu_0$ is the cutoff frequency of the fundamental transverse mode, which is given by $\nu_0=0.58c_0/\mu_0 a$ for a circular metal-clad waveguide, where $a$ is a core diameter. The phase constant $\beta_1$ of the first higher-order transverse ($HE_{21}$, $TE_{01}$, and $TM_{01}$) modes is given by

$$\beta_1=\frac{2\pi\mu_0}{c_0}(\nu^2-\nu_1^2)^{1/2}\ , \tag{3.4}$$

where $\nu_1$ is the cutoff frequency of the first higher-order transverse modes, which is given by $\nu_1=0.75c_0/\mu_0 a$ for a circular metal-clad waveguide. From (3.1), (3.3), and (3.4), the difference in resonant wavelengths $\lambda_0$ and $\lambda_1$ of the fundamental and first higher-order transverse modes is given by

$$\Delta\lambda\equiv\lambda_0-\lambda_1=2\mu_0 d\left[\left[1-\frac{\nu_0^2}{\nu^2}\right]^{1/2}-\left[1-\frac{\nu_1^2}{\nu^2}\right]^{1/2}\right]\ . \tag{3.5}$$

When an optical wavelength is $\lambda=800$ nm ($\nu=3.8\times10^{14}$ s$^{-1}$), the refractive index and thickness of the optical cavity layer are $\mu_0=3.0$ (for AlAs) and $d=114$ nm (half-wavelength), respectively, and the core diameter is $a=0.5$ $\mu$m, then the difference $\Delta\lambda$ is 80 nm. This value is much greater than the microcavity resonant bandwidth of 0.1–1 nm and is also much greater than the spontaneous emission linewidth of 1–30 nm.[16] This means that all the guided modes except the fundamental transverse mode are either in the stop band or outside the stop band, as schematically shown in Fig. 3.

A low-refractive-index buffer layer is inserted between a semiconductor core and a metal cladding to decrease the resistive absorption loss of the fundamental transverse mode. The absorption loss of the fundamental mode is calculated using the Maxwell equations taking into account the complex refractive index of metal.[18,19] For a 500-nm core AlAs slab waveguide with Au cladding, the absorption loss of the fundamental transverse mode is about $10^3$ cm$^{-1}$. If a dielectric buffer layer with refractive index $\mu_b$ and thickness $b$ is inserted between the AlAs core and metal (Au) cladding, the absorption loss is decreased by a factor of

$$\exp[-2b(\beta_0^2-k_0^2n_b^2)^{1/2}]\ , \tag{3.6}$$

where $k_0=2\pi/\lambda$ is the free-space wave number. When

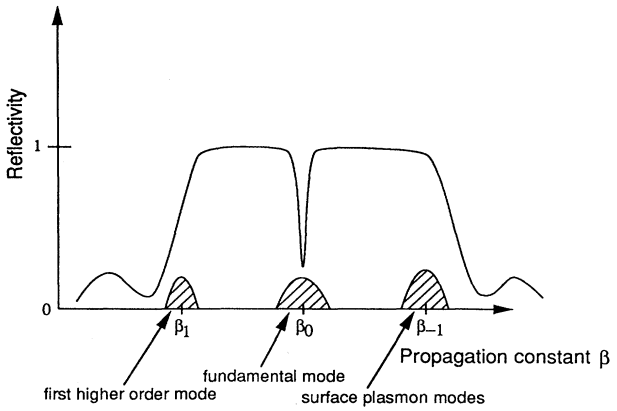


FIG. 3. The reflectivity of the metal-clad waveguide microcavity as a function of the propagation constant. The propagation constants of the surface plasmon modes $\beta_{-1}$, the fundamental mode $\beta_0$, and the first higher-order mode $\beta_1$ have a spread due to the spontaneous emission spectral width.

$\beta_0\simeq3.0k_0$, $n_b=1.38$ (for MgO), and $b=0.1$ $\mu$m, the reduction factor of absorption loss is about $10^{-2}$. Therefore, the absorption loss of the fundamental mode is reduced to about 10 cm$^{-1}$ by such a thin buffer layer. This value is comparable to the background free-carrier absorption loss in GaAs and AlAs. However, a real loss will be larger than the theory predicts, mainly because the metal–buffer-layer boundary roughness scatters the fundamental mode to highly lossy surface-plasmon modes. Much technological progress is needed to realize such a low-loss microcavity.

The vacuum-field intensity of the fundamental transverse mode is enhanced by a factor of $4/(1-R)$ at the antinode and at the resonance by the microcavity, as long as the reduced absorption loss $\alpha_0$ satisfies

$$\alpha_0<\frac{1}{L_{\rm eff}}\ln\frac{1}{R}\ , \tag{3.7}$$

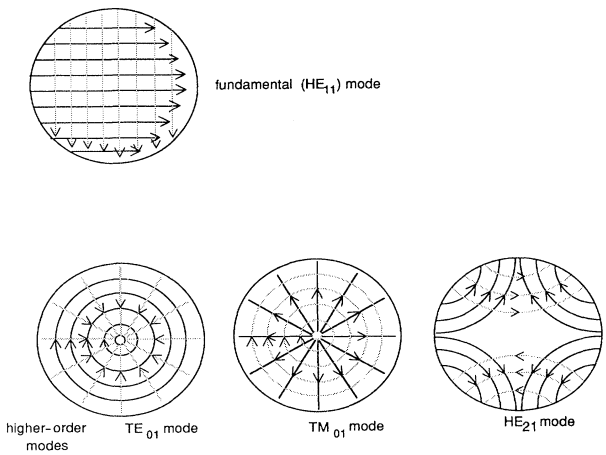


FIG. 4. Electric and magnetic fields of fundamental and higher-order guided modes in a metal-clad circular waveguide with dielectric buffer layer.

where $L_{\text{eff}}$ is the effective cavity length of the microcavity, in which most of the cavity internal field is confined, and $R$ is the reflection coefficient of the DBR. On the other hand, the vacuum-field intensities of all higher-order modes are either suppressed or not altered by the microcavity, because these modes are either in the stop band or outside the stop band of the DBR's. Moreover, higher-order modes have higher absorption loss as a result of the metal cladding, so the resonant enhancement of vacuum-field fluctuation just above the cutoff[3] is smeared out. Therefore, the proposed microcavity structure increases the coupling efficiency of spontaneous emission into the fundamental transverse mode, while keeping those into higher-order modes small or at least unchanged.

If the semiconductor-core region does not have a microcavity structure but rather has a uniform refractive index $\mu_0$, the enhanced or inhibited spontaneous emission is conveniently described by modified density of states rather than modified vacuum-field intensity. The density of states for the fundamental transverse mode is given by[3]

$$\rho_0(\nu)=\frac{4\mu_0}{cA_g}\frac{\nu}{(\nu^2-\nu_0^2)^{1/2}}\simeq\frac{16\nu_0^2\mu_0^3}{\xi c^3}\frac{\nu}{(\nu^2-\nu_0^2)^{1/2}} . \tag{3.8}$$

Here $A_g$ is the cross section of the waveguide and a geometrical factor $\xi$ is $\xi\simeq 1$ for a circular waveguide. The density of states normalized by the free-space value, $\rho_{\text{FS}}(\nu)=8\pi\nu^2\mu_0^3/c^3$, is given by

$$\frac{\rho_0(\nu)}{\rho_{\text{FS}}(\nu)}=\frac{2}{\pi\xi}\left[\frac{\nu_0}{\nu}\right]^2\frac{\nu}{(\nu^2-\nu_0^2)^{1/2}} . \tag{3.9}$$

The normalized density of states is enhanced just above its cutoff $\nu\simeq\nu_0$, as shown in Fig. 5.[3] This is because the fundamental mode just above its cutoff does not propagate along the waveguide, but is almost "trapped" at one position and behaves like a resonator mode. This is the case for microwave superconductor waveguides. However, the guided mode near its cutoff has a fairly large absorption loss at optical frequencies as a result of the metal surface. Consequently, this resonant enhancement of spontaneous emission is not expected at optical frequencies.

On the other hand, if the fundamental mode is well above its cutoff, the absorption loss is decreased but the normalized density of states is also decreased according to (3.9), as shown in Fig. 5. The normalized total density of states for higher-order guided modes is given by[3]

$$\sum_{j\,(\geq 1)}\frac{\rho_j(\nu)}{\rho_{\text{FS}}(\nu)}=\frac{2}{\pi\xi}\left[\frac{\nu_0}{\nu}\right]^2\sum_j\frac{\nu}{(\nu^2-\nu_j^2)^{1/2}} . \tag{3.10}$$

Here $\nu_j$ is the cutoff frequency of mode $j$. In general, (3.10) is larger than (3.9). Equation (3.10) does not go to infinity even at $\nu=\nu_j$, because the higher-order guided mode at just above the cutoff has a large absorption loss due to the metal surface. By choosing the waveguide cross section appropriately, (3.10) can be made smaller than 1. This becomes impossible only if the highest-order guided mode is just above its cutoff. But, otherwise, the total density of states for all guided modes except the fundamental mode can be made smaller than the free-space value,

$$\sum_{j\,(\geq 1)}\frac{\rho_j(\nu)}{\rho_{\text{FS}}(\nu)}<1 . \tag{3.11}$$

Inequality (3.11) is unchanged even if the microcavity structure is introduced in the semiconductor-core region, because all the higher-order modes are either in the stop band or outside the stop band of the DBR's; so the density of states is not enhanced by the microcavity.

On the other hand, the density of states for the fundamental transverse mode is enhanced by the microcavity structure. When the effective reflection coefficient of the DBR's is $R$, the normalized density of states is given by

$$\frac{\rho_0'(\nu)}{\rho_{\text{FS}}(\nu)}=\frac{8}{\pi\xi(1-R)}\left[\frac{\nu_0}{\nu}\right]^2\frac{\nu}{(\nu^2-\nu_0^2)^{1/2}} . \tag{3.12}$$

If the numerical parameters $\lambda=800$ nm, $\mu_0=3.0$, $d=114$ nm, and $a=0.5$ $\mu$m are assumed, then (3.12) reduces to $\rho_0'(\nu)/\rho_{\text{FS}}(\nu)\simeq 0.1/(1-R)$. Since $L_{\text{eff}}$ is on the order of 1 $\mu$m for an AlAs/GaAs microcavity,[16] the inequality (3.7) is satisfied for $R\leq 0.999$. Values of $R=0.95$, 0.99, and 0.999 give $\rho_0'(\nu)/\rho_{\text{FS}}(\nu)\simeq 2$, 10, and 100, respectively. The coupling efficiency of spontaneous emission into the fundamental mode, which is given by

$$\beta=\rho_0'(\nu)\Big/\left[\rho_0'(\nu)+\sum_{j\,(\geq 1)}\rho_j(\nu)\right] , \tag{3.13}$$

is about 0.67, 0.91, and 0.99 for those $R$ values, respectively.

A one-dimensional periodic structure[16] requires a large refractive-index difference between DBR layers to achieve a high coupling efficiency $\beta$ into a single-lasing mode. In the metal-clad optical waveguide microcavity treated here, however, a large refractive index difference is not necessary; instead the coupling efficiency $\beta$ is simply increased by the large $R$ value.

The spontaneous lifetime normalized by that in a homogeneous GaAs is given by

$$\frac{\tau_{\text{sp}}}{\tau_{\text{sp},0}}=\rho_{\text{FS}}(\nu)\Big/\left[\rho_0'(\nu)+\sum_{j\,(\geq 1)}\rho_j(\nu)\right] . \tag{3.14}$$

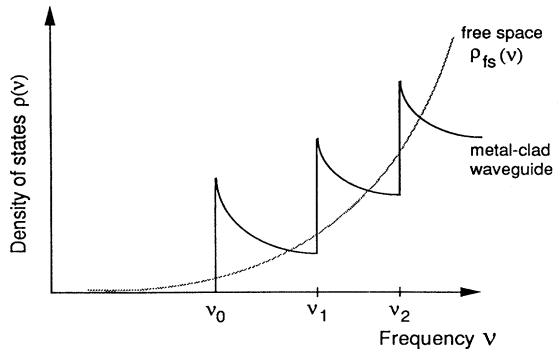


FIG. 5. The densities of states in the metal-clad waveguide and in free space.

This value is 0.33, $10^{-1}$, and $10^{-2}$ for $R=0.95$, 0.99, and 0.999, respectively. Since $\tau_{sp,0}$ is on the order of 3 ns, the spontaneous lifetime can be decreased even to 30 ps. This is in sharp contrast to the one-dimensional periodic structure, in which the spontaneous lifetime is increased rather than shortened.[16]

## IV. CHARACTERISTICS OF MICROCAVITY SEMICONDUCTOR LASERS

In a conventional semiconductor laser, only a very small part of the spontaneous emission is coupled into a single-lasing mode as discussed in Sec. II. The reason is twofold: First, the radiation pattern of spontaneous emission is isotropic, so a substantial part of the spontaneous emission is not coupled to the guided modes in an active waveguide with a small acceptance angle but is coupled to radiation continuum modes propagating in oblique directions. Second, the spontaneous emission spectral linewidth is broader than the longitudinal cavity mode spacing, so a substantial part of the spontaneous emission is not coupled to a lasing guided mode but is coupled to nonlasing guided modes. As discussed already, the coupling efficiency of spontaneous emission into a lasing mode, i.e., spontaneous emission coefficient $\beta$, can be increased to close to 1 for a microcavity semiconductor laser from $10^{-5}$ for a conventional semiconductor laser. The spontaneous lifetime is also decreased to 30 ps for a microcavity semiconductor laser from 3 ns for a conventional semiconductor laser. The characteristics of such a microcavity semiconductor laser are very different from a conventional semiconductor laser.

### A. Basic equations

The quantum Langevin equation for the (total) electron number operator $\hat{N}_c$ is written as[22]

$$\frac{d}{dt}\hat{N}_c = P - \left[\frac{1-\beta}{\tau_{sp}}+\frac{\beta}{\tau_{sp}}\right]\hat{N}_c - (\hat{E}_{cv}-\hat{E}_{vc})\hat{n}+\hat{\Gamma}_p+\hat{\Gamma}_{sp}+\hat{\Gamma}\ , \tag{4.1}$$

where $P$ is the pump rate, $\beta\langle\hat{N}_c\rangle/\tau_{sp}$ is the spontaneous emission rate into a lasing mode, $(1-\beta)\langle\hat{N}_c\rangle/\tau_{sp}$ is the spontaneous emission rate into all other modes except the lasing mode, $\langle\hat{E}_{cv}\rangle$ and $\langle\hat{E}_{vc}\rangle$ are the stimulated emission and absorption rates per photon, $n_{sp}=\langle\hat{E}_{cv}\rangle/(\langle\hat{E}_{cv}\rangle-\langle\hat{E}_{vc}\rangle)$ is a population inversion parameter, and $\hat{n}$ is the (total) photon number operator.

The spontaneous emission rate into the lasing mode and the stimulated emission rate per photon should be equal by the Einstein's relation, so that we have

$$\frac{\beta}{\tau_{sp}}\langle\hat{N}_c\rangle=\langle\hat{E}_{cv}\rangle\ . \tag{4.2}$$

The noise operators associated with the pump process, the spontaneous emission process and the stimulated emission or absorption process satisfy the following correlation functions:

$$\langle\hat{\Gamma}_p(t)\hat{\Gamma}_p(u)\rangle=0\ , \tag{4.3}$$

$$\langle\hat{\Gamma}_{sp}(t)\hat{\Gamma}_{sp}(u)\rangle=\delta(t-u)\frac{\langle\hat{N}_c\rangle}{\tau_{sp}}\ , \tag{4.4}$$

$$\langle\hat{\Gamma}(t)\hat{\Gamma}(u)\rangle=\delta(t-u)(\langle\hat{E}_{cv}\rangle+\langle\hat{E}_{vc}\rangle)\langle\hat{n}\rangle\ . \tag{4.5}$$

Here (4.3) indicates that the pump noise for a semiconductor laser is suppressed by a high-impedance constant current source.[23–26] Equations (4.4) and (4.5) indicate that the spontaneous emission, stimulated emission, and absorption are Poisson point processes, which means one event occurs independently when the previous event occurs.

The quantum Langevin equations for (total) photon number operator $\hat{n}$ is written as

$$\frac{d}{dt}\hat{n}=-\left[\frac{\omega}{Q}-(\hat{E}_{cv}-\hat{E}_{vc})\right]\hat{n}+\frac{\beta}{\tau_{sp}}\hat{N}_c+\hat{F}+\hat{F}_e\ , \tag{4.6}$$

where $\omega/Q$ is the photon decay rate. The noise operators associated with the stimulated emission or absorption process, spontaneous emission process, and the photon decay process satisfy the following correlation functions:

$$\langle\hat{F}(t)\hat{F}(u)\rangle=\delta(t-u)\left[(\langle\hat{E}_{cv}\rangle+\langle\hat{E}_{vc}\rangle)\langle\hat{n}\rangle+\frac{\beta\langle\hat{N}_c\rangle}{\tau_{sp}}\right], \tag{4.7}$$

$$\langle\hat{F}_e(t)\hat{F}_e(u)\rangle=\delta(t-u)\frac{\omega}{Q}\langle\hat{n}\rangle\ . \tag{4.8}$$

Here $\hat{F}_e=2\sqrt{(\omega/Q)\langle\hat{n}\rangle}\hat{f}$, and $\hat{f}$ is the vacuum-field fluctuation amplitude incident on an output coupling mirror. Since $\hat{\Gamma}'$ ($\equiv\hat{\Gamma}+\hat{\Gamma}_{sp}$) and $\hat{F}$ are originally from the same dipole moment noise operator, they are correlated, using (4.2), as

$$\langle\hat{\Gamma}'(t)\hat{F}(u)\rangle=\langle\hat{F}(t)\hat{\Gamma}'(u)\rangle = -\delta(t-u)\times\left[(\langle\hat{E}_{cv}\rangle+\langle\hat{E}_{vc}\rangle)\langle\hat{n}\rangle+\frac{\beta\langle\hat{N}_c\rangle}{\tau_{sp}}\right]. \tag{4.9}$$

The photon flux operator $\hat{N}$ emanating from the output coupling mirror is[27,28]

$$\hat{N}=\frac{\omega}{Q}\hat{n}-\hat{F}_e\ . \tag{4.10}$$

The first term represents the transmitted internal photon number and the second term represents the quantum interference between the transmitted internal coherent excitation $\sqrt{(\omega/Q)\langle\hat{n}\rangle}$ and the reflected vacuum-field fluctuation $\hat{f}$.

### B. Reduction of threshold pump rate

Let us consider the steady-state (average) solutions of (4.1) and (4.6). Using the linearized solutions, $\hat{N}_c=N_{c0}+\Delta\hat{N}_c$ and $\hat{n}=n_0+\Delta\hat{n}$, in (4.1) and (4.6), we obtain

$$P-\frac{N_{c0}}{\tau_{sp}}-\frac{\beta N_{c0}}{\tau_{sp}n_{sp}}n_0=0\ , \tag{4.11}$$

$$-\left[\frac{\omega}{Q}-\frac{\beta N_{c0}}{\tau_{sp}n_{sp}}\right]n_0+\frac{\beta N_{c0}}{\tau_{sp}}=0\ . \tag{4.12}$$

At pump rates above the threshold, the photon decay rate $\omega/Q$ is equal to the net gain $E_{cv}-E_{vc}$ (i.e., the stimulated emission gain-stimulated absorption loss). Thus,

$$\frac{\omega}{Q}=\frac{\beta N_{c0,th}}{\tau_{sp}n_{sp}}\ , \tag{4.13}$$

where $N_{c0,th}$ is the threshold (total) electron number, which is approached by real electron number $N_{c0}$ only when the pump rate is well above the threshold. The threshold condition is usually written as

$$\exp[(g_{th}-\alpha)L]=\frac{1}{R}\ , \tag{4.14}$$

where $g_{th}$ is the gain constant per unit length, $\alpha$ is the absorption coefficient, $L$ is the active layer length, and $R$ is the power reflection coefficient of the end reflectors. Using the relations

$$g_{th}=(1/v)(E_{cv}-E_{vc})$$

and

$$(1/v)[\alpha+(1/L)\ln(1/R)]=\omega/Q$$

in (4.14), we can obtain the threshold condition

$$\frac{\omega}{Q}=(E_{cv}-E_{vc})=E_{cv}/n_{sp}\ . \tag{4.15}$$

The threshold condition (4.15) is obtained by assuming the net growth rate of photons in (4.6) is zero.

At the threshold pump rate, all the pump electrons recombine via spontaneous emission [the pump rate equals the total spontaneous emission rate $(P_{th}=N_{c0,th}/\tau_{sp})$]. The stimulated emission rate $E_{cv}$ by one photon is equal to the spontaneous emission so that

$$E_{cv}=\beta P_{th}\ . \tag{4.16}$$

From (4.15) and (4.16), the threshold pump rate is calculated as

$$P_{th}=\frac{(\omega/Q)n_{sp}}{\beta}\ . \tag{4.17}$$

Note that the threshold pump rate is inversely proportional to the spontaneous emission coefficient $\beta$, if the photon decay rate $\omega/Q$ and the population inversion parameter $n_{sp}$ are constant. This is an important result which suggests that the threshold pump rate can be decreased by increasing $\beta$.

Physical interpretation of (4.17) is straightforward. $P_{th}$ is the number of electrons injected into the active region per second which is equal to number of spontaneous photons generated in all modes per second, so $\beta P_{th}$ is the number of spontaneous photons generated in the lasing mode per second. That is independent of the spontaneous lifetime $\tau_{sp}$, which determines the average waiting time for an electron to emit a photon but does not determine the number of spontaneous photons generated per second. That is, the total number of electrons in the active region is given by $N_{c0}=P_{th}\tau_{sp}$, so the total number of spontaneously emitted photons per second is $N_{c0}/\tau_{sp}=P_{th}$ and the total number of spontaneous photons coupled to the lasing mode is $\beta N_{c0}/\tau_{sp}=\beta P_{th}$. Since the photon lifetime is $Q/\omega$ s, the average number of spontaneously emitted photons staying inside a cavity is given by $n_0=\beta P_{th}Q/\omega$. At the threshold, the net stimulated emission rate, which is given by $(E_{cv}-E_{vc})n_0$, must be equal to the spontaneous emission rate given by $E_{cv}$. This is the definition of oscillation threshold and it is satisfied when $n_0=\beta P_{th}Q/\omega=n_{sp}$, which gives the threshold pump rate (4.17).

A threshold pump rate is usually calculated via the required gain constant per unit length $g_{th}$ using (4.14), i.e., $g_{th}=\alpha+(1/L)\ln(1/R)$. The gain constant is calculated as a function of carrier density by assuming a certain model for the transition matrix element, Fermi–Dirac electron distribution, and the density of electron states. One such example is Stern's improved matrix element and Gaussian approximation of the Helperin-Lax bandtail (SME-GHLBT) model.[20] Once the threshold carrier density is determined, the total carrier number $N_{c0}$ is obtained by multiplying the carrier density with the active volume $V_a$. The spontaneous lifetime $\tau_{sp}$ is also calculated by the same band model and by the argument of detailed balance.[20] The threshold pump rate is then given by $P_{th}=N_{c0}/\tau_{sp}$. According to this conventional procedure, the photon loss constant $\alpha+(1/L)\ln(1/R)=v(\omega/Q)$ can be decreased and the total spontaneous emission rate $N_{c0}/\tau_{sp}$ for achieving a given gain constant $g_{th}=E_{cv}/n_{sp}v$ can be decreased to achieve a low-threshold pump rate. The first factor corresponds to the reduction of $\omega/Q$ and the second factor corresponds to the reduction of $N_{c0}/\tau_{sp}g_{th}=n_{sp}v/\beta$. This is the meaning of (4.17).

From (4.12), the average photon number $n_0$ is

$$n_0=\frac{\beta N_{c0}/\tau_{sp}}{\omega/Q-\beta N_{c0}/\tau_{sp}n_{sp}}\ . \tag{4.18}$$

It is obvious from this equation that the real electron number $N_{c0}$ never reaches the threshold value $N_{c0,th}$ as long as the spontaneous emission coefficient $\beta$ is nonzero. From (4.12), the average electron number $N_{c0}$ is given by

$$N_{c0}=\begin{cases}N_{c0,th}\dfrac{(r+1)-[(r+1)^2-4(1-\beta)r]^{1/2}}{2(1-\beta)}\ , & \beta\neq 1\\ N_{c0,th}\dfrac{r}{1+r}\ , & \beta=1\ ,\end{cases} \tag{4.19}$$

where $r=P/P_{th}$ is the normalized pump rate and $N_{c0,th}=\omega\tau_{sp}n_{sp}/Q\beta$. Using (4.18) in (4.19), the average photon number $n_0$ is

$$n_0 = \begin{cases} n_{sp}\dfrac{(r+1)-[(r+1)^2-4(1-\beta)r]^{1/2}}{2(1-\beta)} \Big/ \left\{1-\dfrac{(r+1)-[(r+1)^2-4(1-\beta)r]^{1/2}}{2(1-\beta)}\right\}, & \beta \neq 1 \\ n_{sp}r, \quad \beta=1 \ . \end{cases} \tag{4.20}$$

If the photon number $n_0$ is larger than one before the carrier density exceeds a transparency point, the stimulated emission rate into a lasing mode exceeds the spontaneous emission rate into the lasing mode, even though the net gain is still negative. The threshold condition (4.17) holds when the photon number $n_0$ is much smaller than one at the transparency point.[29]

Figure 6 shows the internal photon number $n_0$ versus the pump rate $P$ as a function of the spontaneous emission coefficient $\beta$. It is assumed that $\omega/Q=10^{12}$ s$^{-1}$ and $n_{sp}=1$. To create the ideal population inversion $n_{sp}=1$ in semiconductors, a certain carrier density $n_c=N_{c0}/V_a$ is required. In other words, the population inversion parameter $n_{sp}$ in (4.17) depends on the pump rate. For a GaAs bulk material at room temperature and at 77 K this required carrier density $n_c$ is about $10^{18}$ and $10^{17}$ cm$^{-3}$, respectively.[20] If the pump rate required for realizing the transparency given by

$$P_{PI}=\frac{n_c V_a}{\tau_{sp}} \tag{4.21}$$

is much smaller than the threshold pump rate (4.17), the population inversion parameter at the threshold is $n_{sp}\approx 1$ and the result shown in Fig. 6 is correct. Note that the pump rate $P_{PI}$ is decreased by decreasing the active volume $V_a$ for a given $n_c$ value. In Fig. 6, the active area diameter for a GaAs quantum well with 100 Å thickness that satisfies the population inversion condition is plotted as a function of the pump current $I=qP_{PI}$, where $n_c=10^{18}$ cm$^{-3}$ and $\tau_{sp}=1$ ns are assumed. The threshold pump current $I_{th}\equiv qP_{th}$ is on the order of 10 mA for a conventional semiconductor laser with $\beta\simeq 10^{-5}$. The threshold pump current decreases with decreasing a cavity volume $V$. As shown in Eq. (2.10), $\beta$ is inversely proportional to $V$. $\beta$ can be increased to $10^{-3}$–$10^{-4}$ in a small volume (edge emitting) semiconductor laser without requiring a cavity quantum electrodynamics (QED) effect, for which the expected threshold current is 0.1–1 mA. The threshold current becomes less than 1 $\mu$A for a microcavity semiconductor laser with $\beta\simeq 0.1$–1. The active area diameter must be smaller than 1 $\mu$m to create the population inversion by such a small injection current at room temperature. The size of the active region is incidentally on the same order for the size required to increase the spontaneous emission only into a fundamental guided mode. In the limit of $\beta=1$, the change in differential quantum efficiency from $\eta_D=\beta$ to $\eta_D=1$ disappears. The threshold pump rate defined by (4.17), at which the average internal photon number is $n_0=n_{sp}$, corresponds to the threshold pump current $I_{th}=160$ nA for $\beta=1$, $n_{sp}=1$, and $\gamma=10^{12}$ s$^{-1}$. At pump rates below this value, spontaneous emission is dominant. At pump rates above this value, stimulated emission is dominant. Figure 7 shows the average electron number $N_{c0}$ versus the pump current, where $\tau_{sp}=1$ ns is assumed. In Fig. 7 the active area diameter to realize the population inversion, i.e., $n_c=10^{18}$ cm$^{-3}$, is plotted as a function of $N_{c0}$.

Let us mention here that the threshold condition (4.17) correctly describes the material properties dependence via $n_{sp}$ and $\beta$. For instance, the population inversion parameter $n_{sp}$ for a given pump rate decreases with decreasing a temperature, because the required carrier density for transparency decreases. Note that (4.17) is a self-

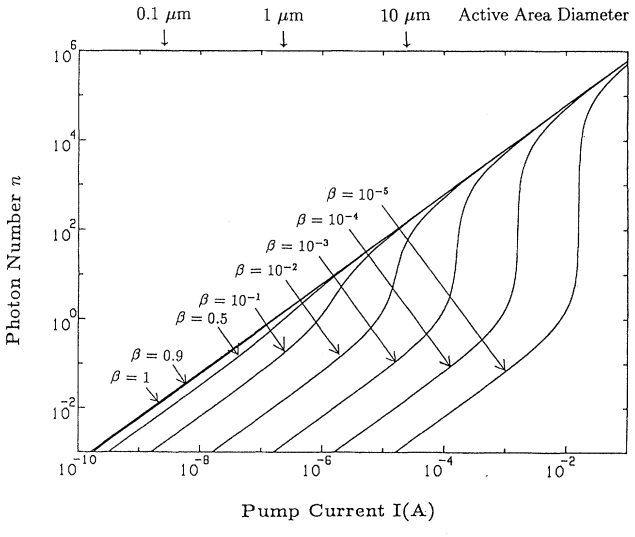


FIG. 6. Internal photon number $n_0$ and required active area diameter vs pump current $I$ as a function of spontaneous emission coefficient $\beta$. $n_{sp}=1$, $\tau_{sp}=10^{-9}$ s and $\omega/Q=10^{12}$ s$^{-1}$.

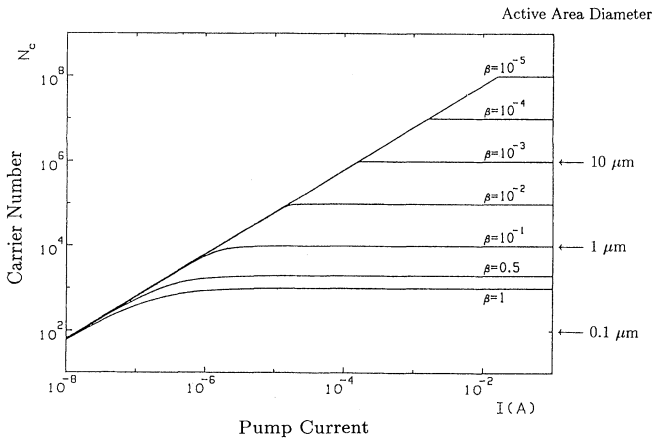


FIG. 7. Electron number $N_{c0}$ vs pump current $I$ as a function of spontaneous emission coefficient $\beta$. $n_{sp}=1$, $\omega/Q=10^{12}$ s$^{-1}$, and $\tau_{sp}=10^{-9}$ s.

consistent relation in which $n_{sp}$ is a function of $P_{th}$. The spontaneous emission coefficient $\beta$ increases by quantum wire or dot structures, because the gain spectral width $\Delta\lambda$ is decreased in such microstructures.

### C. Increase in modulation bandwidth

Since the spontaneous lifetime $\tau_{sp}$ can be decreased by a factor of $10^2$ in a microcavity semiconductor laser, the response for direct intensity modulation via injection current becomes very broad even for a light-emitting diode (LED) operating below the oscillation threshold. When $\tau_{sp}$ is 30 ps as estimated in Sec. III, the modulation bandwidth is $f_c=1/2\pi\tau_{sp}\simeq 5.3$ GHz. Moreover, the quantum efficiency of such a microcavity LED is $\beta\simeq 0.1$ to 1 which is comparable to or higher than that of a conventional semiconductor laser. An even broader modulation bandwidth is expected for a microcavity semiconductor laser operating above the oscillation threshold.

When the pump rate is sinusoidally modulated as $P_0+\Delta P e^{i\Omega t}$, the response of the internal photon number modulation is evaluated by (4.1) and (4.6). The power spectrum of $\Delta n$ is

$$S_{\Delta n}(\Omega)=\frac{[(1+r)/\tau_{sp}]^2}{\Omega^4+\Omega^2\{[\gamma/(1+r)]^2+[(1+r)/\tau_{sp}]^2-(2r\gamma/\tau_{sp})\}+\gamma^2[(1+r)/\tau_{sp}]^2}(\Delta P)^2 . \tag{4.22}$$

Figure 8 shows the normalized power spectrum as a function of the normalized pump rate. The modulation response is dependent on $\gamma\equiv\omega/Q$, $\tau_{sp}$, and $r$, but is independent of $\beta$. When $r\equiv P/P_{th}>(\omega/Q)\tau_{sp}$, (4.22) reduces to

$$S_{\Delta n}(\Omega)\simeq\frac{(\Delta P)^2}{(\omega/Q)^2}\frac{1}{1+(Q/\omega)^2\Omega^2+(Q/\omega)^2(\tau_{sp}^2/r^2)\Omega^4} . \tag{4.23}$$

The relaxation oscillation is shifted beyond the cavity cutoff frequency $\Omega_c=\omega/Q$, and the modulation bandwidth is equal to the cavity cutoff frequency. Since $P_{th}$ is given by (4.17), the pump rate satisfying this ultimate modulation bandwidth is

$$P>P_{th}\frac{\omega}{Q}\tau_{sp}=\frac{(\omega/Q)^2\tau_{sp}n_{sp}}{\beta} . \tag{4.24}$$

When $\gamma=10^{12}$ s$^{-1}$, $\tau_{sp}=10^{-9}$ s, $n_{sp}=1$, and $\beta=1$, pump rate $P$ must be greater than $10^{15}$ (s$^{-1}$), which corresponds to the pump current of 160 $\mu$A. If the pump rate satisfies this condition, the modulation bandwidth is as high as $f_c=(\omega/Q)/2\pi\simeq 160$ GHz.

The physical reason for such an enormous increase in the modulation bandwidth of a microcavity laser is that the electron lifetime is greatly shortened by the stimulated emission process. The internal field strength interacting with dipoles produced by a single photon increases with decreasing a cavity volume.

### D. Amplitude squeezing

It was theoretically and experimentally demonstrated that the photon flux fluctuation from a semiconductor laser can be reduced to below the shot-noise level (amplitude squeezing).[23–26] As shown in Fig. 9, the output photon flux fluctuation from an ordinary laser having shot-noise-limited pump fluctuation approaches the shot-noise level at pump rates far above threshold, while that from a constant-current-driven semiconductor laser

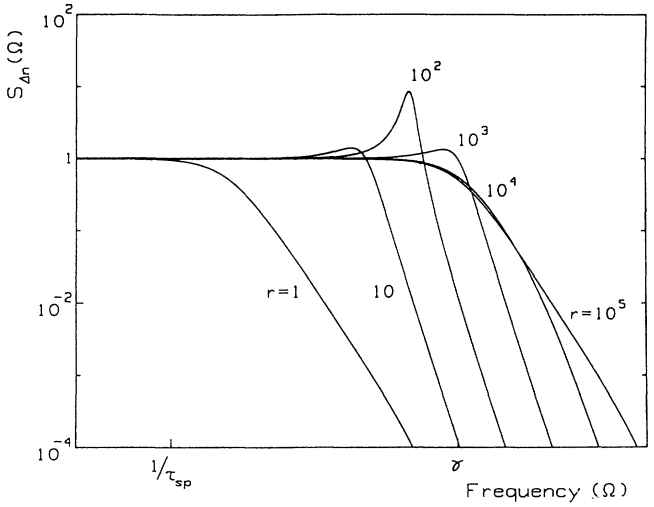


FIG. 8. Normalized intensity modulation response $S_{\Delta n}(\Omega)$ as a function of pump rate $r=P/P_{th}$.

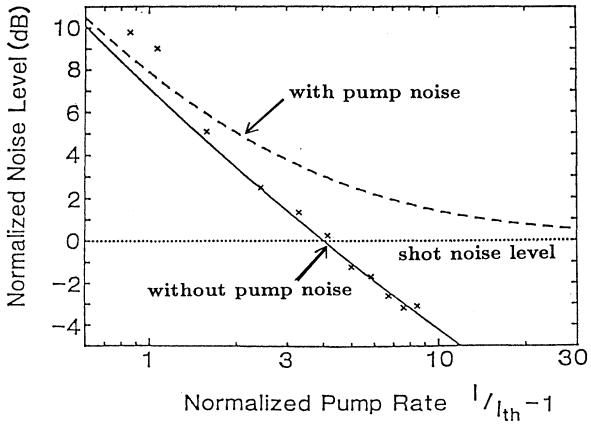


FIG. 9. The normalized photon flux fluctuation level vs pump rate. Solid and dashed lines are theoretical results and crosses are experimental results.

having no pump fluctuation is reduced to below the shot-noise level. However, the photon flux fluctuation at pump rates near the threshold is not reduced to below the short-noise level, because the spontaneous emission is randomly coupled into the laser mode which is amplified rather than attenuated at near the threshold. This problem can be solved if the spontaneous emission coefficient $\beta$ is increased close to unity and the randomness of spontaneous photon coupling is eliminated.

The small fluctuation operators $\Delta\hat{N}_c$ and $\Delta\hat{n}$ obey

$$\frac{d}{dt}\Delta\hat{N}_c=-\frac{1}{\tau_{sp}}\left[1+\frac{\beta n_0}{n_{sp}}\right]\Delta\hat{N}_c - \frac{\beta N_{c0}}{\tau_{sp}n_{sp}}\Delta\hat{n}+\hat{\Gamma}_p+\hat{\Gamma}_{sp}+\hat{\Gamma}\ , \tag{4.25}$$

$$\frac{d}{dt}\Delta\hat{n}=-\left[\frac{\omega}{Q}-\frac{\beta N_{c0}}{\tau_{sp}n_{sp}}\right]\Delta\hat{n} + \frac{\beta}{\tau_{sp}}\left[1+\frac{n_0}{n_{sp}}\right]\Delta\hat{N}_c+\hat{F}+\hat{F}_e\ . \tag{4.26}$$

The Fourier-transformed photon number fluctuation operator is

$$\Delta\tilde{n}=\frac{A_4(\tilde{\Gamma}_p+\tilde{\Gamma}_{sp}+\tilde{\Gamma})-(j\Omega+A_1)(\tilde{F}+\tilde{F}_e)}{A_2A_4-(j\Omega+A_1)j\Omega+A_1)(j\Omega+A_4)}\ . \tag{4.27}$$

Here the tilde denotes the Fourier-transformed operator and the coefficients are

$$A_1=\frac{1}{\tau_{sp}}\left[1+\frac{\beta n_0}{n_{sp}}\right]\ , \tag{4.28}$$

$$A_2=\frac{\beta N_{c0}}{\tau_{sp}n_{sp}}\ , \tag{4.29}$$

$$A_3=\frac{\omega}{Q}-\frac{\beta N_{c0}}{\tau_{sp}n_{sp}}\ , \tag{4.30}$$

$$A_4=\frac{\beta}{\tau_{sp}}\left[1+\frac{n_0}{n_{sp}}\right]\ . \tag{4.31}$$

Using the boundary condition (4.10), the Fourier-transformed photon flux fluctuation operator becomes

$$\Delta\tilde{N}=\left\{\frac{\omega/Q}{A_4}(\tilde{\Gamma}_p+\tilde{\Gamma}_{sp}+\tilde{\Gamma})-(j\Omega+A_1)\frac{\omega}{Q}\tilde{F} - \left[\Omega^2-\left[A_1A_3-A_2A_4+\frac{\omega}{Q}A_1\right]-j\Omega\left[A_1+A_3-\frac{\omega}{Q}\right]\right]\tilde{F}_e\right\}\Big/[\Omega^2-(A_1A_3-A_2A_4)-j\Omega(A_1+A_3)]\ . \tag{4.32}$$

The power spectrum is

$$S_{\Delta\tilde{N}}(\Omega)=2\left\{\frac{\omega}{Q}A_4^2\left[\frac{(\omega/Q)n_{sp}}{\beta}+\frac{\omega}{Q}(2n_{sp}-1)n_0\right]+\left[\frac{\omega}{Q}\right]^2(\Omega^2+A_1^2+2A_1A_4)\left[\frac{\omega}{Q}n_{sp}+\frac{\omega}{Q}(2n_{sp}-1)n_0\right] + \left\{\left[\Omega^2-\left[A_1A_3-A_2A_4+\frac{\omega}{Q}A_1\right]\right]^2+\Omega^2\left[A_1+A_3-\frac{\omega}{Q}\right]^2\right\}\frac{\omega}{Q}n_0\right\} \times\{[\Omega^2-(A_1A_3-A_2A_4)]^2+\Omega^2(A_1+A_4)^2\}^{-1}\ . \tag{4.33}$$

Figure 10 shows the normalized power spectral density $S_{\Delta\tilde{N}}(\Omega)/2N_0$ in the limit $\Omega\to 0$ as a function of the normalized pump rate $r$ for various $\beta$ values. When the spontaneous emission coefficient $\beta$ is on the order of $10^{-5}$, the output photon flux fluctuation is reduced to below the shot-noise level only at high pump rates. However, if the spontaneous emission coefficient $\beta$ is close to 1, the output photon flux fluctuation is reduced to below the shot-noise level at pump rates even very close to the threshold. The output photon flux fluctuation is reduced to below the shot-noise limit also at pump rates below the threshold. A conventional LED has a very small coupling efficiency of spontaneous emission, so that strong sub-Poissonian statistics of injected electrons are smeared out by a random deletion process and end up with very weak sub-Poissonian statistics of emitted photons. The increased $\beta$ value by a microcavity solves this problem.

Figure 11 shows the normalized photon flux fluctuation spectra as a function of the pump rate for a special

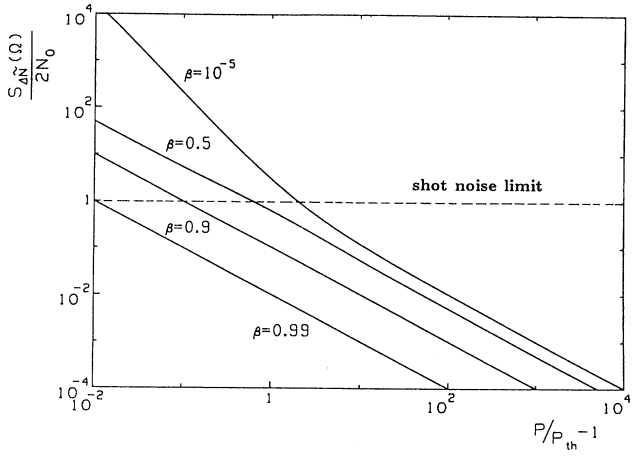


FIG. 10. Normalized photon flux spectral density as a function of normalized pump rate $P/P_{th}-1$.

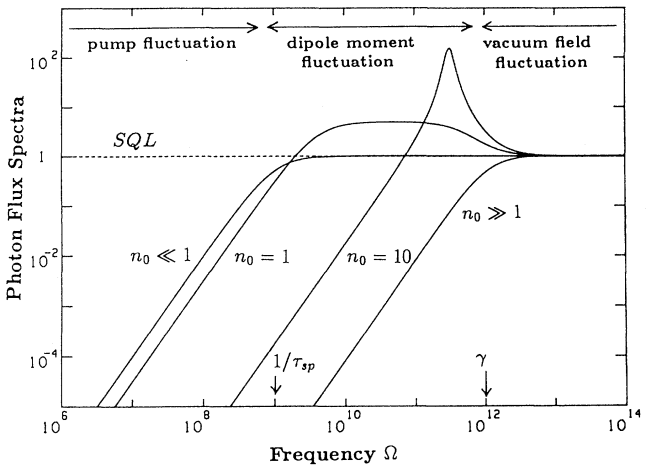


FIG. 11. Normalized photon flux spectra for $\beta=1$ as a function of internal photon number $n_0$.

case of $\beta=1$. The output photon flux fluctuation is reduced to below the shot-noise level at all pump rates including below, near, and above the threshold.

The physical reason for this change is obvious from the energy conservation argument. If the spontaneous emission coefficient $\beta$ is unity, all the injected electrons emit photons in a single mode that are extracted from the cavity sooner or later. Therefore, if the output photon number is counted for a time interval much longer than the delay time involved in the electron-photon conversion process and in the photon escaping process, the output photon number is constant because the input electron number is constant. The time constant is the spontaneous lifetime $\tau_{sp}$ at a pump rate far below the threshold, and is the photon lifetime $Q/\omega$ at a pump rate far above the threshold. On the other hand, when the spontaneous emission coefficient $\beta$ is much smaller than unity, the conversion efficiency from the injected electrons to the emitted photons jumps suddenly at the threshold, where the output photon number becomes very noisy.

## V. CONCLUSION

The microcavity semiconductor laser can concentrate all the spontaneous emission power into a single cavity-resonant mode and achieve near-unity quantum efficiency of spontaneous emission. $\beta$ is roughly the inverse of the number of modes, so it can be automatically increased inversely with a cavity volume without requiring the principle of cavity QED. Cavity QED plays an important role if a cavity designer manages to selectively increase the spontaneous emission rate into a lasing mode and decrease those into nonlasing modes. In such a well-designed cavity, $\beta$ increases faster than the inverse of the number of modes which is determined by the cavity volume. The spontaneous lifetime can also be reduced by a factor of 100. The characteristics of such a semiconductor laser can be altered drastically. The microcavity semiconductor laser is a surface-emitting light source that has high quantum efficiency, a low threshold pump rate, high-speed response, and low noise. Potential applications include ultrahigh-speed optical communications, optical connections in a large-scale-integrated circuit (LSI), and two-dimensional optical information processing.

It is important to realize the spontaneous emission linewidth be narrower than the cavity resonant linewidth. Then, the requirement for the active volume for realizing ideal population inversion is relaxed. A possible "exciton laser"[30] is one candidate for meeting this requirement. A "quantum wire" or "quantum dot" laser[31] is another candidate.

[1]E. M. Purcell, Phys. Rev. **69**, 681 (1946).
[2]K. H. Drexhage, in Progress in Optics, edited by E. Wolf (North-Holland, New York, 1974), Vol. 12, pp. 165–232.
[3]D. Kleppner, Phys. Rev. Lett. **47**, 233 (1981).
[4]P. Goy, J. M. Raimond, M. Gross, and S. Haroche, Phys. Rev. Lett. **50**, 1903 (1983).
[5]G. Gabrielse and H. Dehmelt, Phys. Rev. Lett. **55**, 67 (1985).
[6]R. G. Hulet, E. S. Hilfer, and D. Kleppner, Phys. Rev. Lett. **55**, 2137 (1985).
[7]F. De Marttini, G. Innocenti, G. R. Jacobovitz, and P. Mataloni, Phys. Rev. Lett. **59**, 2955 (1987).
[8]W. Jhe, A. Anderson, E. A. Hinds, D. Meschede, L. Moi, and S. Haroche, Phys. Rev. Lett. **58**, 666 (1987).
[9]D. J. Heinzen, J. J. Childs, J. E. Thomas, and M. S. Feld, Phys. Rev. Lett. **58**, 1320 (1987).
[10]E. Yablonovitch, T. J. Gmitter, and R. Bhat, Phys. Rev. Lett. **61**, 2546 (1988).
[11]R. J. Glauber and M. Lewenstein, Phys. Rev. A **43**, 467 (1991).
[12]T. Kobayashi, T. Segawa, A. Morimoto, and T. Sueta (unpublished).
[13]Y. Yamamoto, S. Machida, K. Igeta, and Y. Horikoshi, in *Coherence and Quantum Optics VI*, edited by L. Mandel, E. Wolf and J. H. Eberly (Plenum, New York, 1990).
[14]H. Yokoyama and S. D. Brorson, J. Appl. Phys. **66**, 4801 (1989).
[15]E. Yablonovitch, Phys. Rev. Lett. **58**, 2059 (1987).
[16]G. Björk, K. Igeta, S. Machida, and Y. Yamamoto, following paper, Phys. Rev. A **43**, 669 (1991).
[17]H. Yokoyama, S. D. Brorson, E. P. Ippen, K. Nishi, and T. Anan, IEEE J. Quantum Electron. **QE-26**, 1492 (1990).
[18]T. Takano and J. Hamasaki, IEEE J. Quantum Electron. **QE-8**, 206 (1972).
[19]Y. Yamamoto, T. Kamiya, and H. Yanai, IEEE J. Quantum Electron. **QE-11**, 729 (1975).
[20]H. C. Casey, Jr. and M. B. Panish, *Heterostructure Lasers* (Academic, New York, 1978), Chap. 3.
[21]Y. Suematsu and K. Furuya, Trans Inst. Electron. Commun. Eng. Jpn. **E-60**, 467 (1977).
[22]H. Haug, Phys. Rev. **184**, 338 (1969).
[23]Y. Yamamoto, S. Machida, and O. Nilsson, Phys. Rev. A **34**, 4025 (1986).
[24]Y. Yamamoto and S. Machida, Phys. Rev. A **35**, 5114 (1987).
[25]S. Machida, Y. Yamamoto, and Y. Itaya, Phys. Rev. Lett. **58**,

1000 (1987).
[26]S. Machida and Y. Yamamoto, Phys. Rev. Lett. **60**, 792 (1988).
[27]Y. Yamamoto and N. Imoto, IEEE J. Quantum Electron. **QE-22**, 2032 (1986).
[28]O. Nilsson, S. Machida, and Y. Yamamoto, IEEE J. Quantum Electron. **QE-22**, 2043 (1986).
[29]G. Björk and Y. Yamamoto, IEEE J. Quantum Electron. (to be published).
[30]T. T. J. M. Berendschot, H. A. J. M. Reinen, and H. J. A. Bluyssen, Appl. Phys. Lett. **54**, 1827 (1989).
[31]Y. Arakawa and H. Sakaki, Appl. Phys. Lett. **40**, 939 (1982).